THERMAL BEHAVIOUR OF FLUIDIZED BEDS DIRECTLY IRRADIATED BY A CONCENTRATED SOLAR RADIATION

Claudio Tregambi*, Riccardo Chirone**, Fabio Montagnaro***, Piero Salatino*, Roberto Solimene**

claudio.tregambi@unina.it

*Dipartimento di Ingegneria Chimica, dei Materiali e della Produzione Industriale, Università degli Studi di Napoli Federico II, Piazzale Vincenzo Tecchio 80, 80125 Napoli (Italy).
**Istituto di Ricerche sulla Combustione, Consiglio Nazionale delle Ricerche, Piazzale Vincenzo Tecchio 80, 80125 Napoli (Italy).
***Dipartimento di Scienze Chimiche, Università degli Studi di Napoli Federico II, Complesso Universitario di Monte Sant'Angelo, 80126 Napoli (Italy).

Abstract
Directly-irradiated fluidized bed reactors are very promising in the context of concentrated solar power applications as they can be operated at process temperatures high enough to perform thermochemical storage with high energy density. The present study aims at experimentally investigating the direct interaction between a concentrated simulated solar radiation and a fluidized bed by measuring the time-resolved bed surface temperature with an infrared camera under different fluidization gas velocities. The effect of a localized generation of bubbles was investigated too, by injecting a chain of bubbles through a nozzle located just at the centre of the concentrated solar beam. The obtained results encourage the localized generation of bubbles, just at the larger value of the impinging radiative heat flux, as a strategy to reduce the overheating of the bed surface and, as a consequence, the energy losses related to fluidizing gas and radiative re-emission.
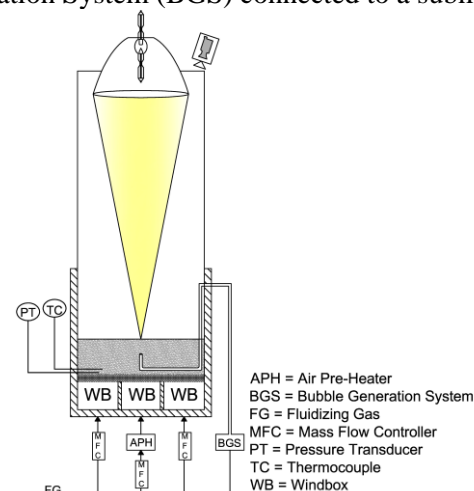
Introduction
Development and deployment of Concentrating Solar Power (CSP) as a renewable energy resource is gaining ever-increasing interest as this represents a key climate-change mitigation technology. CSP plants coupled with thermodynamic cycles can be more reliable and flexible than other renewable resources, as they can be integrated with Thermal Energy Storage (TES) systems to overcome the intrinsic sunlight variability [1]. The gas–solid fluidized bed technology has been proposed for the development of solar receivers characterized by large heat transfer coefficients and thermal diffusivities [2–3]. The potentialities of such reactors have already been recognized in the past by several authors [2, 4–6]. More recently, fluidized beds have been tested in the generation of solar fuels at laboratory scale [7–8] and they have been also proposed as a promising technology for the

integration of post-combustion CO_2 capture and storage technique with CSP [9]. The external surface of fluidized beds can be directly irradiated by concentrated solar radiation (direct heating) or, differently, the solar radiation can be focused on a cavity transferring the heat to the fluidized bed reactor by conduction through the external wall (indirect heating). A direct absorption of the solar energy allows high operating temperatures, but has to face problems to keep the fluidized bed column or the window clean (scratches-free) [6]. On the other hand, indirect heating of fluidized beds decreases the feasible process operation temperatures and increases the thermo-mechanical stresses acting on the solar irradiated wall of the reactor but no scratches or transmittance problems do however exist for such configuration.

The present study aims at experimentally investigating the direct interaction of a concentrated simulated solar radiation with the bed surface of a fluidized bed. Bed surface overheating is a critical issue because it determines the efficiency of fluidized beds as thermal receivers. A fluidized bed filled by SiC particles was directly irradiated by a highly concentrated solar simulated radiation. The interaction between the fluidized particles moving under the action of bubble bursting and the concentrated solar radiation was analysed by the time-resolved bed surface temperature varying the mean fluidization gas velocity. The effect of a localized generation of bubbles was also investigated injecting a chain of bubbles through a nozzle located just at the centre of the concentrated solar beam.

Experimental Apparatus and Materials

The experimental apparatus used in the present work is schematized in Figure 1. It mainly consists of: **i)** a fluidized bed reactor with a gas preheater and a mass flow control system; **ii)** a temperature and pressure measurement system of the bottom bed; **iii)** a solar simulator composed by a short-arc Xe lamp and an optical reflector; **iv)** an infrared camera to measure the bed surface temperature; **v)** a discrete Bubble Generation System (BGS) connected to a submerged nozzle.

APH = Air Pre-Heater
BGS = Bubble Generation System
FG = Fluidizing Gas
MFC = Mass Flow Controller
PT = Pressure Transducer
TC = Thermocouple
WB = Windbox

Figure 1. Schematic of the experimental apparatus and its ancillary equipment.

The fluidized bed column has an internal square cross section of 0.78 m and an height of 0.6 m. The windbox, 0.2 m high, is compartmented in three independent sections fed by three mass flow meters of 200 $Nm^3 h^{-1}$ each. J-type thermocouples and piezoresistive pressure transducers are located nearby the distributor to monitor the bed temperature and the fluidization conditions, respectively. The Xe-lamp used for the solar simulator is an ozone-free model with a 4 kW_{el} power, while the reflector is an elliptical-shaped model because of its capability of concentrate the radiations coming from its first focal point into a second fixed focal point. The solar simulator was able to produce a concentrated beam with a peak flux of 1100 kW m^{-2} in the focal point. The infrared camera (Optris PI-400) was coupled with a tele-lens to measure the temperature in an observation window of 0.35×0.26 m at a distance of 1.5 m, and with a pixel resolution of 0.9 mm. Two calibration ranges are used during image acquisition: 0–250 and 200–1500 °C. The discrete BGS is composed of a cylinder–piston system connected to the submerged nozzle (8 mm ID), through which bubbles are injected inside the bed. The system was optimized to generate bubbles at a frequency of 1 Hz and with a mean diameter of 0.065 m. The increase of fluidization velocity due to the BGS system is negligible if the total cross section of the fluidized bed is considered. Air was used as fluidizing gas, and SiC (Size Range: 50–350 μm; Sauter Mean Diameter: 0.127 mm) as solid bed material, mainly because of its dark colour (good solar absorber).

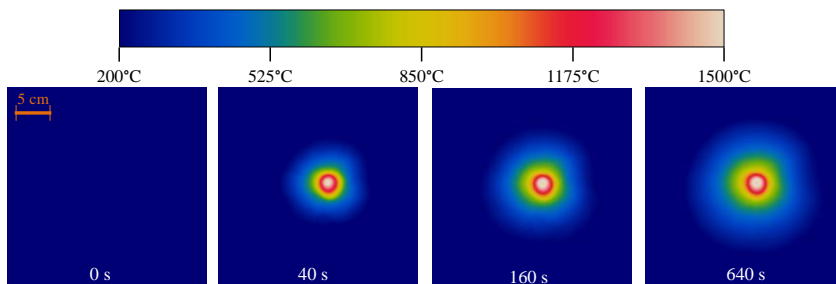**Experimental Procedure and Operating Conditions**
The lamp beam was focused at the centre of the upper surface of the fluidized bed. Before each test, the bed was preheated up to a temperature of 30 °C. Once the set temperature was reached, time-resolved thermal images of the bed surface were continuously acquired by the infrared camera at a sampling frequency of 27 Hz and, then, the Xe lamp was turned on. Experiments were carried out under different inlet gas velocities, from fixed bed to vigorously fluidized bed conditions, namely from 0 to 0.1 m s^{-1}. Each test lasted about 15 minutes. The camera calibration range used for data acquisition was chosen following the experimental needs: a lower calibration range was used when the fluidization velocity was increased. Additional tests were performed using the BGS and following the same procedure previously described. The submerged nozzle was arranged inside the fluidized bed and aligned with the focal point of the solar simulated radiation. The influence of both the bed inlet gas velocity and the bed surface–nozzle distance was investigated, while the bubble generation frequency was always kept at 1 Hz. Two values of the bed surface–nozzle distance were investigated: 0.09 m and 0.03 m. The former distance was chosen to give the bubbles enough space to completely grow before bursting, while the latter distance was selected to have formation and eruption of the bubbles at the same time.
The acquired thermal images were post-processed to obtain the time-averaged temperatures and standard deviations of the measurement point (pixel size) located at the focus of the beam on which the maximum flux of 1100 kW m^{-2} impinges

("central point", from now on). Every test was finally checked for the data congruency, which was always verified. Only the steady state condition data were analysed to calculate the mean values and standard deviations.
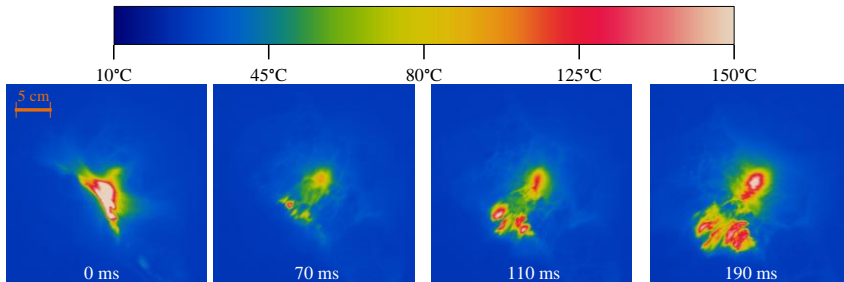
Results and Discussion
Figure 2 shows a thermal images sequence of the bed surface captured under fixed bed conditions (no fluidizing fed to the bed). The frame at 0 s correspond to the time instants just before the lamp was turned on. It is noteworthy that, being the adopted infrared camera calibration range 200–1500 °C, the dark blue colour refers to 200 °C and lower temperatures, while the white colour corresponds to 1500 °C and higher temperatures. The analysis of Figure 2 shows the establishment of the fingerprint of the simulated solar radiation on the bed surface with time. It is evident a central hot zone corresponding to larger radiative heat flux, whose temperature and area extension increase with time. After only 40 s from lamp ignition, temperatures of over 1500 °C were obtained in the central zone, while after 160 s, in the central zone (white and red colours in the pictures), bed surface temperature appears quite steady. For longer times, the simulated solar radiation only determines a moderate temperature increase in the region surrounding the central one. The central hot zone approached a circular region of about 0.006 m, and it was characterized by white colour indicating that the maximum temperature detectable by the thermal camera was achieved, thus the temperature was actually larger than 1500 °C.

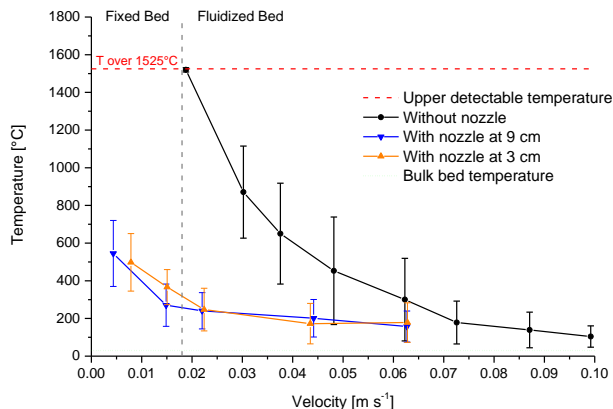**Figure 2.** Thermal images of bed surface under fixed bed conditions.

Figure 3 reports a sequence of thermal images of the upper surface of the fluidized bed under gently fluidized bed conditions (0.073 m s^{-1}). The sequence refers to a time-window shorter than those previously reported, because the bubble eruption phenomena which rule the time-variability of the bed surface temperature are characterized by shorter time-scales. The analysis of the sequence highlights that bubble bursting reduces the overheating of the bed surface area corresponding to the maximum impinging radiative heat flux. More specifically, Figure 3 shows the mechanism of ejection and displacement of the hot particles heated by the high radiative flux toward the surrounding regions due to bubble bursting. On the whole, at such fluidizing gas velocities, the bubble eruption frequency provides a continuous renewal of the fluidized bed surface, even if it is possible to observe a

slight overheating in some limited time lapse between two successive eruption events. Indeed, bubbles are not always formed in the close proximity of the central hot zone, and few seconds without particle renewal are enough to let the temperature steeply increases.

Figure 3. Thermal images of bed surface at a superficial gas velocity of 0.073 m s^{-1}.

Figure 4 reports the time-averaged bed surface temperature with standard deviations as a function of the superficial gas velocity. The standard deviation values are representative of the temperature fluctuations, and are not related to the measurement error. Concerning the data obtained without using the BGS it is possible to observe that: **a)** when the gas velocity is lower than the fluidization value, the bed surface temperatures are higher than 1500 °C and an increase in the superficial gas velocity produces only slight or none improvements in terms of mean temperature reduction; **b)** as soon as the superficial gas velocity exceeds the minimum fluidization value, a steep decrease of the bed surface temperature is evident; **c)** increasing the fluidization velocity, the mean temperatures progressively decrease toward the bed bulk temperature, whereas the standard deviation values initially grow up and then, after having reached a maximum value at a superficial gas velocity of about 0.05 m s^{-1}, begin to decrease.

Figure 4. Time-averaged bed surface temperature with standard deviations, as a function of the superficial gas velocity.

Observing instead the data obtained using the BGS, it is easy to recognize the beneficial role of the BGS in the reduction of the bed surface temperature. The temperatures achieved are indeed strongly lower than the corresponding values obtained at the same superficial gas velocity but without the BGS. The obtained results encourage the localized generation of bubbles, just at the larger value of the impinging radiative heat flux, as a strategy to reduce the overheating of the bed surface and, as consequence, the energy losses related to fluidizing gas and to radiative re-emission. This strategy can be also applied to preserve the chemico-physical properties of reactive materials involved in high-temperature thermochemical cycles.

Acknowledgments

References

[1] Pardo, P., Deydier, A., Anxionnaz-Minvielle, Z., Rougé, S., Cabassud, M., Cognet, P., "A review on high temperature thermochemical heat energy storage", *Renew. Sust. Energ. Rev.* 32: 591–610 (2014).

[2] Bachovchin, D.M., Archer, D.H., Neale, D.H., "Heat transfer in a fluidized-bed solar thermal receiver", *AIChE Symp. Ser.* 79: 27–36 (1983).

[3] Solimene, R., Fenelli, P., Chirone, R., Salatino, P., "Heat transfer phenomena in bubbling fluidized beds for concentrated solar power", *Proc 11th International Conference on Fluidized Bed Technology*, Beijing, China, pp 435–440.

[4] Flamant, G., Hernandez, D., Bonet, C., Traverse, J.P., "Experimental aspects of the thermochemical conversion of solar energy; Decarbonation of $CaCO_3$", *Sol. Energy* 24: 385–395 (1980).

[5] Flamant, G., Olalde, G., "High temperature solar gas heating comparison between packed and fluidized bed receivers–I", *Sol. Energy* 21: 463–471 (1983).

[6] Koenigsdorff, R., Kienzle, P., "Results of and prospects for research on direct-absorption fluidized bed solar receivers", *Sol. Energ. Mater.* 24: 279–283 (1991).

[7] von Zedtwitz, P., Lipiński, W., Steinfeld A., "Numerical and experimental study of gas-particle radiative heat exchange in a fluidized-bed reactor for steam-gasification of coal", *Chem. Eng. Sci.* 62: 599–607 (2007).

[8] Gokon, N., Izawa, T., Kodama, T., "Steam gasification of coal cokes by internally circulating fluidized-bed reactor by concentrated Xe-light radiation for solar syngas production", *Energy* 79: 264–272 (2015).

[9] Tregambi, C., Montagnaro, F., Salatino, P., Solimene, R., "A model of integrated calcium looping for CO_2 capture and concentrated solar power", *Sol. Energy* 120: 208–220 (2015).